



# New determination of the thermophysical properties of argon gas considering nuclear spin and symmetry effects

F. Bouchelaghem<sup>1</sup> · H. Boutarfa<sup>2</sup> · M. Chicouche<sup>1</sup> · S. Lias<sup>3</sup>

Received: 6 May 2025 / Accepted: 1 July 2025

© The Author(s), under exclusive licence to Springer-Verlag GmbH Germany, part of Springer Nature 2025

## Abstract

**Context** Since statistical physics and quantum mechanics were first successfully combined thanks in part to the work of Chapman and Cowling and Hirschfelder. Extensive theoretical and experimental research has been dedicated to understanding the kinetics of gases and gas mixtures. This integration has, among other achievements, theoretically established a direct link between the macroscopic properties of gases whether measured or calculated and the quantum characteristics of their constituent particles. This model successfully established straightforward mathematical relationships linking the microscopic interactions between the atomic and/or molecular components of a gas to measurable transport properties, such as diffusion and viscosity coefficients. It also provided explanations for how these properties vary and how they are influenced by thermodynamic parameters like pressure, density, and temperature.

**Methods** The potential data available to us are either obtained from ab initio calculations or experimental measurements. The ab initio values of the potential  $V(R)$  are derived from a quantum-theoretical approach to the molecular problem. Typically, these methods provide the potential energy at discrete values of the internuclear distance  $R$  within a specified range. To build the potential energy curve corresponding to the fundamental interactions, we will rely on ab initio data. Knowing this potential allows for the numerical solution of the radial wave equation using Numerov's method, ultimately enabling the calculation of the phase shifts  $\eta(E)$ . From the elastic collision phase shifts, we derive the self-diffusion coefficient  $D$ , viscosity  $\eta$ , and thermal conductivity  $\lambda$  using the Chapman-Enskog model. For diffusion and viscosity, we perform calculations both with accounting for the symmetry and spin effects associated with the identical nature of the colliding particles. We then examine how these transport coefficients vary with temperature and propose a straightforward computational approach to obtain analytical expressions for  $D(T)$ ,  $\eta(T)$ , and  $\lambda(T)$ .

**Keywords** Ab initio potential · Second virial coefficient · Diffusion coefficient · Viscosity and conductivity

## Introduction

Atomic collisions are fundamentally important in atomic physics and molecular. They are able to adequately describe

Multiscale simulation and materials modeling, Materials and renewable energy laboratory.

✉ F. Bouchelaghem  
fouzia.bouchelaghem@univ-msila.dz

<sup>1</sup> Physics Department, Mohamed Boudiaf University, University Pole, Road Bourdj Bou Arreiridj, 28000 M'sila, Algeria

<sup>2</sup> Physics Department, Chadli Bendjedid University, 36000 El Taref, Algeria

<sup>3</sup> Physics Department, University Houari Boumediene, Bab Ezzouar, 16000 Algiers, Algeria

the kinetics of gases and their hydrodynamic properties. They are thus important in the interpretation of some phenomena of astrophysics, quantum chemistry, and laser physics and plasma. We are interested in this study of purely elastic atom-atom collisions in a gas. As we will see, such collisions can lead to thermophysical properties and their behavior with temperature. Combining statistical physics with quantum mechanics and by the works of Chapman and Colling [1] and Hirschfelder et al. [2], tremendous efforts, theoretical and empirical, have been devoted to the study of the kinetics of gases and gas mixtures [2, 3]. This combination has, among other things, highlighted in a purely theoretical way the direct correlation between macroscopic properties, measured or calculated, and quantum characteristics of gas constituents. The Chapman-Enskog model [1, 2] for dilute gases, proposed in the 1920 for the integration of the Boltzmann equation, is a

good example of the success of such an approach. This model was able to establish simple mathematical relationships between the interactions that prevail at the microscopic scale between the different atomic and/or molecular constituents of a gas and some generally measurable transport properties, such as diffusion, viscosity, and conductivity coefficients. In this work, we have set as goal to analyze some thermophysical properties of argon gas as described by the Chapman-Enskog model. The work is mainly motivated by the fact that specific and recent potentials relating to the Ar–Ar dimer have been made available to the scientific community. More particularly, the transport coefficients will be revisited at low and high temperatures by considering the symmetry effect.

Atomic units (a.u.) are used throughout this paper, unless otherwise stated.

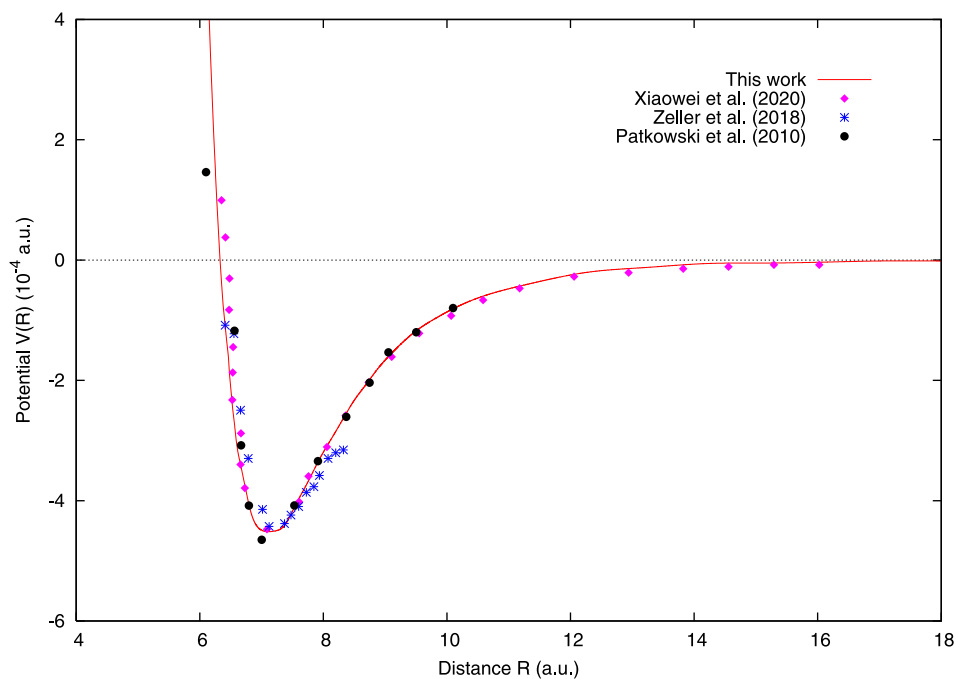
## Interaction potential

The interaction of two argon atoms Ar(1s) – Ar(1s) in the ground state occurs according to the unique molecular symmetry  ${}^1\Sigma_g^+$ , the interaction potential  $V(R)$  between two atoms is generally constructed in three distinct areas: intermediate distances,  $R_S \leq R \leq R_L$ ; short distances,  $0 < R \leq R_S$ ; and great distances,  $R_L \leq R < \infty$ .

### Intermediate distances

For intermediate distances, we use the values of potential energies obtained in the literature, between  $R = R_S$  and  $R = R_L$ . In order to construct this molecular state of Ar<sub>2</sub>,

**Fig. 1** Potential-energy curves of Ar<sub>2</sub>. The curves are compared with published data from Sheng et al. [5], Zeller et al. [9], and Patkowski et al. [8]



we used 63 *ab initio* energy values of Pitrov et al. [4] for  $1.13a_0 \leq R \leq 18.89a_0$ . The data has led to a potential for well depth  $D_e = -0.4525 \times 10^{-3}$  a.u. at equilibrium distance  $R_e = 7.110$  a.u. These spectroscopic data are comparable to  $D_e = -0.45 \times 10^{-3}$  a.u. at  $R_e = 7.10$  a.u. of Sheng et al. [5] and with spectroscopic data  $D_e = -0.4523 \times 10^{-3}$  a.u. at  $R_e = 7.119$  a.u. of Patkowski et al. [6].

### Short distances

For  $R \leq 1.13a_0$ , we use the analytical expression of Born-Mayer

$$V(R) \sim A \exp(-\alpha R), \quad (1)$$

where the potential  $V(R)$  and its first derivative  $dV(R)/dR$  are continuous at point  $R = R_S$ , and then get these parameters easily.

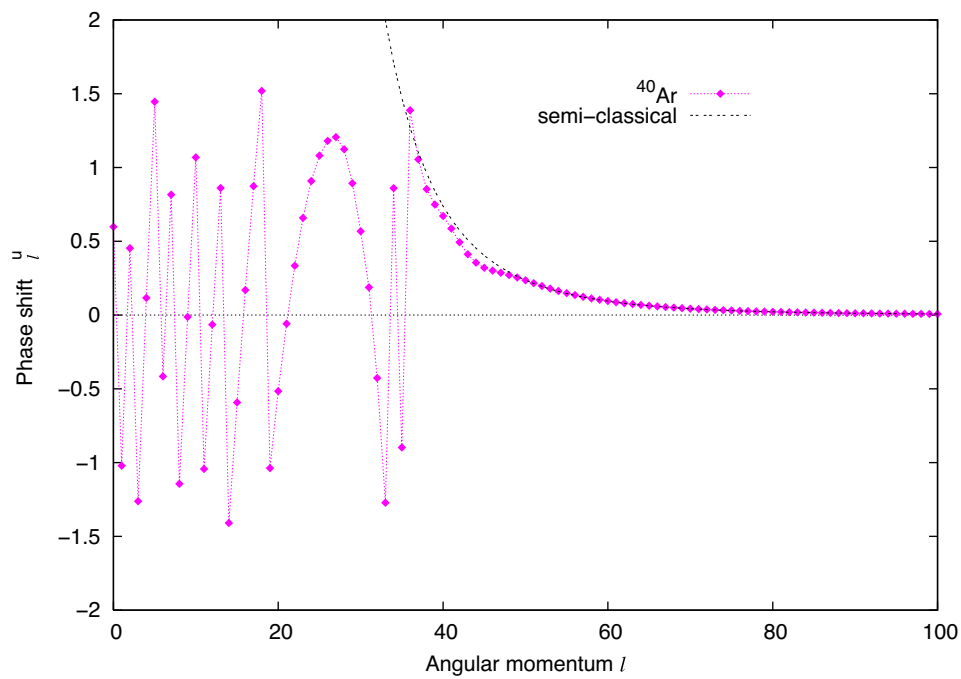
$$\alpha = \frac{-dV(R)/dR}{V(R)} \Big|_{R=R_S} \quad (2)$$

and

$$A = V(R) \exp(+\alpha R) \Big|_{R=R_S}. \quad (3)$$

Our calculations give us the values of  $A = 155.440$  and  $\alpha = 1.937$ . These values are deducted digitally following a smooth connection with the data of the intermediate part.

**Fig. 2** Phase shift  $\eta_l(E)$  to the energy  $E = 10^{-4}$  u.a. of Ar



## Great distances

Beyond  $R = 18.89a_0$ , the interaction potential is generally attractive. It can be expressed in terms of inverse powers of  $R$  [7]

$$V(R) = -\frac{C_6}{R^4} - \frac{C_8}{R^6} - \frac{C_{10}}{R^8}, \quad (4)$$

where the constant coefficients  $C_6 = 64.2890$ ,  $C_8 = 1514.86$ , and  $C_{10} = 50240$  in (a.u.) are called dispersion coefficients taken from [8].

The potential energy curve thus constructed is shown in Fig. 1 compared to data published by Sheng et al. [5], Zeller et al. [9] and Patkowski et al. [6], where good agreement with these authors is observed.

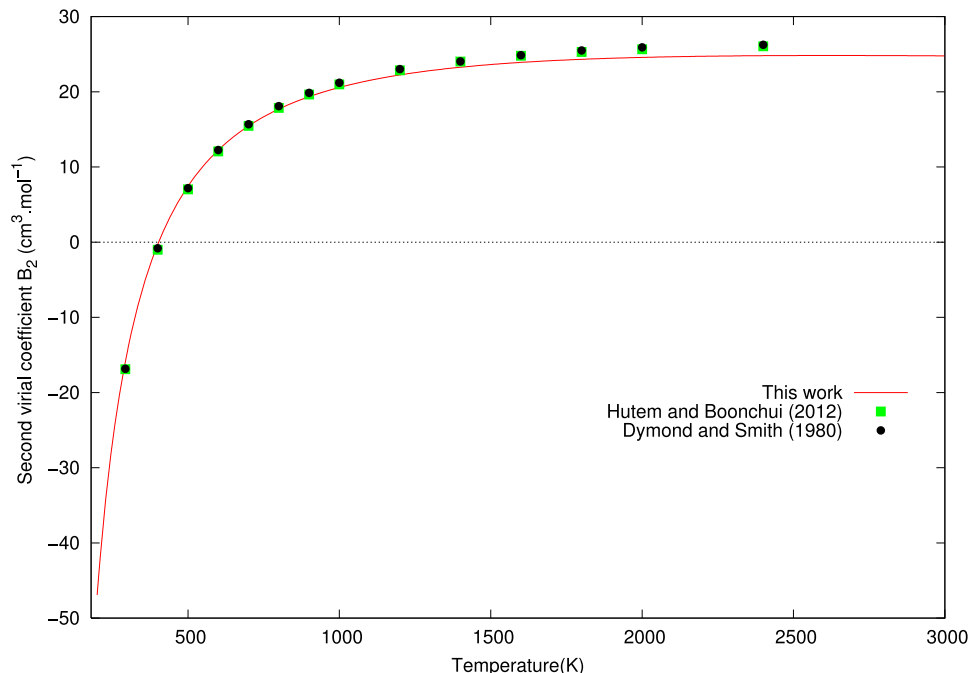


**Fig. 3** Second virial coefficient as a function of temperature  $T$  compared with published data from Hutem and Boonchui [13] and Dymond and Smith [14]

## Phase shift calculation

Having properly determined the interatomic potential  $V(R)$ , it is now possible to numerically solve the Schrödinger radial equation [3, 10]

$$\left[ \frac{d^2}{dR^2} + k^2 - 2\mu V(R) - \frac{l(l+1)}{R^2} \right] u_l(R) = 0. \quad (5)$$

In quantum mechanics, the  $u_l(R)$  solution of this equation will have asymptotic behavior

$$u_l(R) \sim \sin \left( kR - \frac{l}{2}\pi + \eta_l \right). \quad (6)$$

Using the Numerov algorithm [11], the Fortran code we developed enables the calculation of the phase shifts  $\eta_l(E)$  for each energy  $E$  and orbital angular momentum  $l$ . These phase shifts are essential for determining the hydrodynamic properties of an  $\text{Ar}_2$  gas and their temperature-dependent behavior. The calculation of  $\eta_l(E)$  is made for all energies between  $E_{\min} = 10^{-6}$  u.a. and  $E_{\max} = 10^{-1}$  u.a. with the maximum value of the orbital kinetic moment  $l_{\max} = 1000$ . The calculations are performed quantically up to a certain value of  $l = l_{\text{sc}}$ , beyond which the program is forced to use the approximate semi-classical phase shift given by the form

$$\eta_l \simeq \frac{3\pi}{16} \mu C_6 \frac{k^4}{l^5}. \quad (7)$$

Figure 2 shows the phase shift  $\eta_l$  at an energy of  $E = 10^{-4}$  u.a. The shape of the asymptotic form (7) is also shown in the same figure.

## The second virial coefficient

One of the physical means available to verify the quality and accuracy of the potential that we have previously constructed, there is the evaluation of the second virial coefficient  $B_2(T)$  and analysis of their behavior with temperature  $T$ . It is well known in chemistry-physics [2, 12] that the thermodynamic properties of a real gas monoatomic, density  $n$ , pressure  $p$ , and temperature  $T$ , can be described by the equation of state

$$\frac{p}{k_B T} = n + B_2(T)n^2 + B_3(T)n^3 + \dots \quad (8)$$

The various coefficients  $B$  is called virial coefficients and  $B_i$  are the coefficients of virial. If the higher terms corresponding to  $i \geq 2$  are neglected, the equation of state (8) becomes that of a perfect gas where there is total absence of any mutual interaction between the atoms that make up the

gas under consideration. For sufficiently diluted gases, i.e., low density, the virial coefficients of orders higher may be omitted to have

$$\frac{p}{k_B T} = n + B_2(T)n^2. \quad (9)$$

From this expression, it appears that the second virial coefficients, expressed by mechanics statistics as a function of interatomic potential [12]

$$B_2(T) = -\frac{1}{2} \int [\exp(-V(\mathbf{R})/k_B T) - 1] d^3\mathbf{R}, \quad (10)$$

represent the deviation of the actual gas from its ideal behavior when collision binaries are heavily involved  $V(R)$ . In

**Table 1** Diffusion coefficients  $D(T)$

Temperature	$D (10^{-4}\text{m}^2\text{s}^{-1})$	Ref. [19]	Ref. [17]
T/K	( $n = n_0$ )	( $p = p_0$ )	
1	13.95[-2]	51.15[-5]	
50	0.31[-1]	0.58[-2]	
80	0.049	0.014	
100	0.061	0.022	0.022
150	0.090	0.049	0.049
200	0.11	0.086	0.086
273	0.155	0.155	0.154
293	0.164	0.176	0.183
300	0.168	0.184	0.185
313	0.174	0.199	0.196
350	0.190	0.244	0.245
400	0.212	0.312	0.311
450	0.232	0.383	0.384
500	0.251	0.461	0.463
600	0.288	0.634	0.637
700	0.323	0.827	0.833
800	0.355	1.041	1.048
900	0.386	1.272	1.283
1000	0.416	1.523	1.536
2000	0.673	4.933	4.990
3000	0.891	9.793	9.939
4000	1.089	15.952	16.230
5000	1.274	23.339	23.775
6000	1.452	32.300	32.513
7000	1.624	42.124	41.636
8000	1.792	52.497	53.396
9000	1.956	64.485	65.478
10,000	2.119	77.613	78.619

Numbers in square brackets are powers of 10

**Table 2** Viscosity  $\eta$  and conductivity  $\lambda$ , varying with temperature  $T$ 

Temperature $T/K$	$\eta$ ( $\mu\text{Pa} \cdot \text{s}$ )	[18]	[19]	[21]	$\lambda$ ( $\text{mW/mK}$ )	[18]	[19]	[21]
1	0.195				0.152			
30	2.839	2.861			2.215	2.236		
50	4.300	4.319		4.32	3.355	3.375		3.38
84	6.863	6.871			5.113	5.355		
100	8.122	8.127	8.128	7.97	6.337	6.344	6.336	6.22
150	12.081	12.085	12.075	11.94	9.426	9.432	9.425	9.32
200	15.876	15.875	15.860	15.89	12.387	12.387	12.374	12.41
273	20.955					16.349	15.142	15.23
300	22.697	22.691	22.673	22.83	17.709	17.726	17.712	17.83
350	25.753		25.736		20.093		20.112	
400	28.616	28.630	28.613		22.326	22.382	22.368	
450	31.315		31.333		24.432		24.503	
500	33.876	33.936	33.921		26.431	26.546	26.534	
600	38.667	38.788	38.574		30.169	30.354	30.344	
700	43.113	43.300	43.036		33.637	33.896	33.887	
800	47.296	47.549	47.540		36.901	37.232	37.224	
900	51.273		51.581		40.004		40.396	
1000	55.844	55.458	55.451		42.977	43.438	43.432	
1500	72.435		72.998		56.515		57.191	
2000	87.956	88.609	88.610		68.625	69.4248	69.425	
3000	115.54	116.550	116.56		90.150	91.306	91.311	
4000	140.01		141.83		109.24		111.09	
5000	162.52	165.374	165.38		126.80	129.521	129.53	
6000	183.82		187.70		143.41		146.99	
7000	204.36		209.07		159.45		163.71	
8000	224.51		229.69		175.16		179.83	
9000	244.61		249.68		190.84		195.47	
10,000	265.04	269.156	269.16		206.79	210.700	210.70	

this case, the potential  $V(R)$  has a spherical symmetry. One easily obtains from Eq. (10)

$$B_2(T) = -2\pi \int_0^\infty \left[ e^{-V(R)/k_B T} - 1 \right] R^2 dR. \quad (11)$$

Our calculated values of second virial coefficient  $B_2(T)$ , corresponding to high temperatures ranging from  $T = 200$  to  $3000$  K, are shown in Fig. 3. The results are compared with theoretical values obtained by Hutem and Boonchui [13] and experiment values of Dymond and Smith [14]; the agreement is good. For a certain temperature,  $T = T_B$  called Boyle's temperature, the coefficients  $B_2(T = T_B) = 0$ . In this case, the second virial coefficient  $B_2(T) = 2.701 \times 10^{-7}$  (cm<sup>3</sup>/mol) at Boyle's temperature  $T_B = 406$  K, it is close to the result that Hutem and Boonchui [13] found, which is  $B_2(T) = 8.856 \times 10^{-7}$  (cm<sup>3</sup>/mol) at  $T_B = 410.151$  K.

## Transports coefficients

### Diffusion and viscosity coefficients

According to the Chapman-Enskog method, the diffusion coefficient  $D$  of a gas, diluted and monoatomic, of density  $n_1$  in another gas, diluted and monoatomic, of density  $n_2$  is equal to [1–3]

$$D(T) = \frac{3}{8(n_1 + n_2)} \left( \frac{\pi k_B T}{2\mu} \right)^{1/2} \frac{1}{\Omega^{(1,1)}(T)}, \quad (12)$$

where  $\Omega^{(1,1)}(T)$  so-called *integrals collision* of diffusion

$$\Omega^{(1,1)}(T) = \frac{1}{2(k_B T)^3} \int_0^\infty E^2 \sigma_D(E) \exp(-E/k_B T) dE, \quad (13)$$

Generally,  $n_1$

$\ll$

$n_2$ , where  $n_2 = n$ , Eq. 12 can be simplified to the following form

$$D(T) \simeq \frac{3}{8n} \left( \frac{\pi k_B T}{2\mu} \right)^{1/2} \frac{1}{\Omega^{(1,1)}(T)}. \quad (14)$$

if  $n_1 \equiv 0$ , the diffusion coefficient is called *self-diffusion* coefficient. The diffusion coefficient expressed by formulas (12) and (14) is given as a function of density. It is also possible to calculate the diffusion coefficients at a given pressure  $p$ , using the ideal gas law  $p = nk_B T$ .

The coefficient of viscosity  $\eta$  is given at temperature  $T$ , by [2]

$$\eta(T) = \frac{5}{16} \frac{\sqrt{2\mu\pi k_B T}}{\Omega^{(2,2)}(T)} \quad (15)$$

where  $\Omega^{(2,2)}(T)$  so-called *integrals collision* of viscosity

$$\Omega^{(2,2)}(T) = \frac{1}{4(k_B T)^4} \int_0^\infty E^3 \sigma_V(E) \exp(-E/k_B T) dE. \quad (16)$$

$\sigma_D(E)$ ,  $\sigma_V(E)$  are diffusion and viscosity cross sections. In quantum mechanics, it is appropriate to consider the nuclear

spin and the symmetry effect that is due to the indiscernability of atoms colliding in the gas [2]. The cross sections of diffusion and viscosity, symmetrical ( $S$ ) and antisymmetrical ( $A$ ), are [15, 16]

$$\sigma_D = \frac{s+1}{2s+1} \sigma_D^{(S)} + \frac{s}{2s+1} \sigma_D^{(A)} \quad (17)$$

where

$$\sigma_D^{(S)}(E) = \frac{8\pi}{k^2} \sum_{l \text{ even}} (2l+1) \sin^2 \eta_l \quad (18)$$

$$\sigma_D^{(A)}(E) = \frac{8\pi}{k^2} \sum_{l \text{ odd}} (2l+1) \sin^2 \eta_l. \quad (19)$$

and

$$\sigma_V = \frac{s+1}{2s+1} \sigma_V^{(S)} + \frac{s}{2s+1} \sigma_V^{(A)} \quad (20)$$

where

$$\sigma_V^{(S)} = \frac{8\pi}{k^2} \sum_{l \text{ even}} \frac{(l+1)(l+2)}{(2l+3)} \sin^2(\eta_{l+2} - \eta_l) \quad (21)$$

$$\sigma_V^{(A)} = \frac{8\pi}{k^2} \sum_{l \text{ odd}} \frac{(l+1)(l+2)}{(2l+3)} \sin^2(\eta_{l+2} - \eta_l). \quad (22)$$

In the case of  $^{40}\text{Ar}$  ( $s = 0$ ).

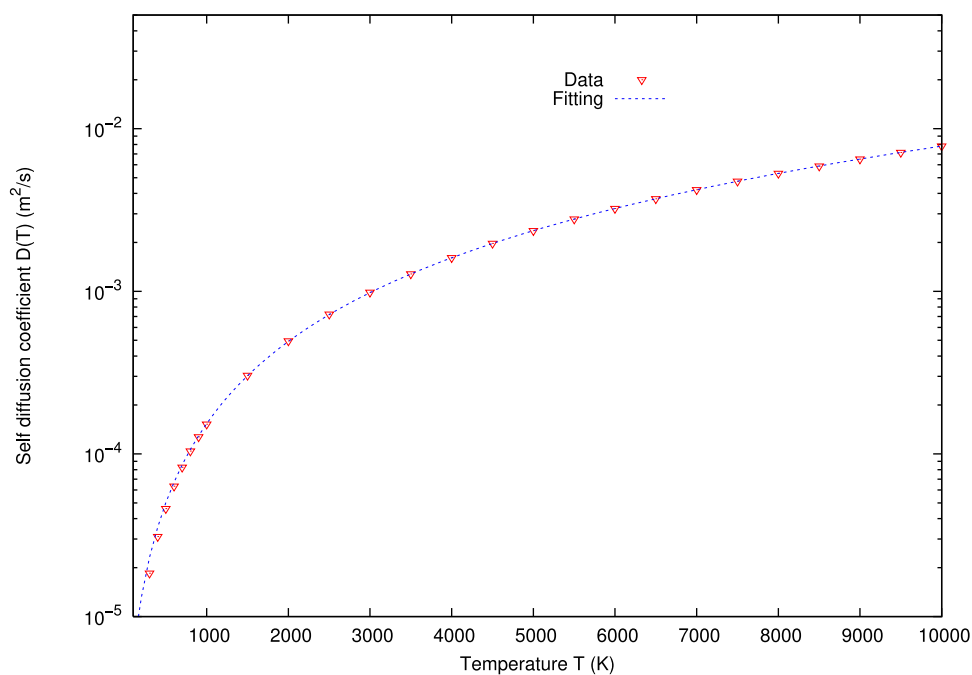
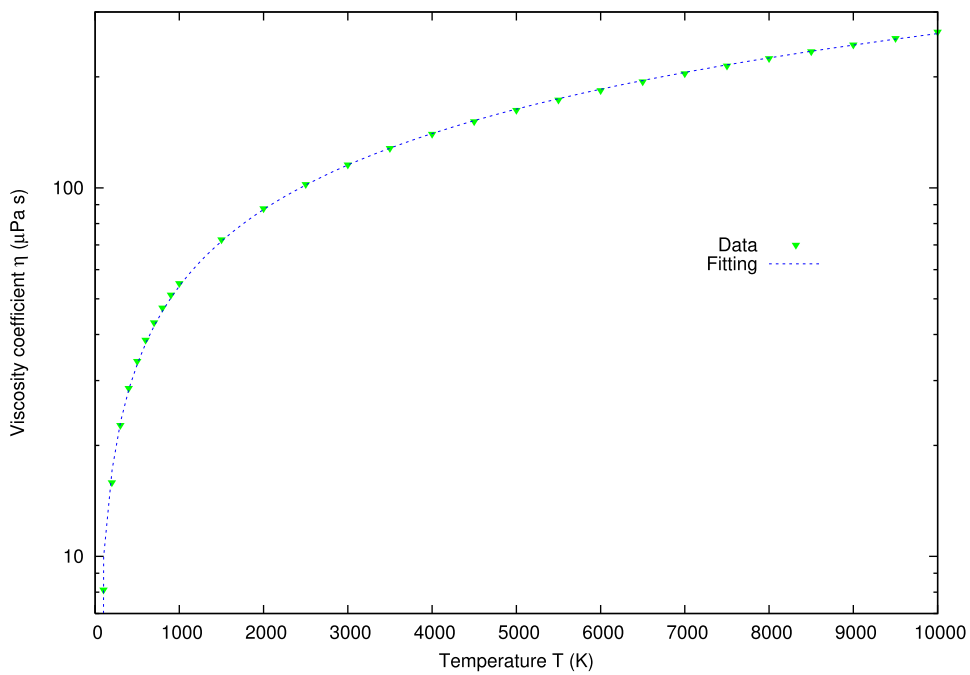


**Fig. 4** Fitting data of self-diffusion coefficient

**Fig. 5** Fitting data of viscosity coefficient



## Conductivity coefficient

Knowledge of the coefficient of viscosity  $\eta$  allows the coefficient of thermal conductivity  $\lambda$  to be deduced. This coefficient is related to  $\eta(T)$  by the formula

$$\lambda(T) = \frac{5}{4} \frac{C_v}{\mu} \eta(T) \quad (23)$$

where  $C_v$  is the specific heat per atom assumed, in general, to be  $3k_B/2$  for monoatomic gases [2]. If we refer to the

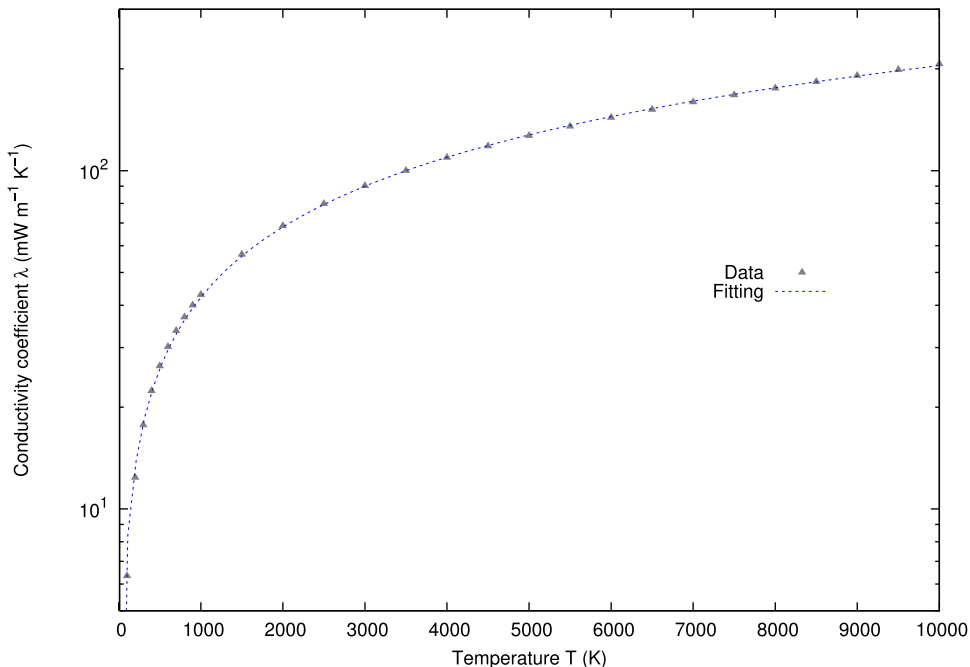
molar mass  $m$  of the chemical species forming the gas under consideration, it comes.

$$\lambda(T) = \frac{15}{4} \frac{R}{m} \eta(T). \quad (24)$$

with  $R \simeq 8.315 \text{ J mol}^{-1} \text{ K}^{-1}$  being the molar constant of the gases.

Our calculations of the self-diffusion coefficient  $D(T)$  at temperature region from  $T=1 \text{ K}$  to  $T=10,000 \text{ K}$  are presented

**Fig. 6** Fitting data of conductivity coefficient



in Table 1. These results are given for density  $n_0 = 2.686 \times 10^{25} \text{ m}^{-3}$  and gas pressure  $p_0 = 101.325 \text{ kPa}$ . Our values are compared in the table with those obtained by Ghimire and Adhikari [17] and Song et al. [19], we also found in particular at  $T = 273 \text{ K}$ , the value of  $D = 0.155 \text{ cm}^2 \text{ s}^{-1}$  which is similar to experimental value  $0.157 \text{ cm}^2 \text{ s}^{-1}$  of McQuarrie [20].

Moreover, our results of the coefficients of viscosity  $\eta(T)$  and thermal conductivity  $\lambda(T)$  are presented in the Table 2 and compared with some values published at temperature region from  $T = 1 \text{ K}$  to  $T = 10,000 \text{ K}$ . The agreement of our values with the data of Sharipov and Benites [18], Song et al. [19], and Kestin et al. [21] is generally good. In addition, we found for  $T = 273 \text{ K}$ , the value of  $\eta = 20.90 \text{ } (\mu\text{Pa} \cdot \text{s})$  et  $\lambda = 16.31 \text{ (mW/mK)}$  that are similar to experimental values  $\eta = 21 \text{ } (\mu\text{Pa} \cdot \text{s})$ ,  $\lambda = 16.3 \text{ (mW/mK)}$  of [22].

We have also used our data on diffusion  $D(T)$ , viscosity  $\eta(T)$ , and conductivity  $\lambda(T)$  coefficients to determine their law of variation with temperature  $T$ . We have for this purpose used the functions

$$\begin{aligned} D(T) &\sim AT^\zeta \exp(-\xi/T) \\ \eta(T) &\sim BT^\zeta \exp(-\xi/T) \\ \lambda(T) &\sim CT^\zeta \exp(-\xi/T) \end{aligned}$$

to fit our values of  $D$ ,  $\eta$ , and  $\lambda$  in the temperature range between 100 and 10,000 K. If  $\eta$  is in  $\mu \text{ Pas}$ ,  $\lambda$  in  $\text{mW m}^{-1} \text{ K}^{-1}$  and  $T$  in K, the algorithm we used generates the constant parameters for diffusion  $A = 8.520 \times 10^{-10} \pm 2.093 \times 10^{-11}$ ,  $\zeta = 1.739 \pm 0.002$ ,  $\xi = -85.885 \pm 14.11$  for viscosity  $B = 0.504 \pm 0.020$ ,  $\zeta = 0.679 \pm 0.004$ ,  $\xi = 15.870 \pm 8.377$ , for conductivity  $C = 0.393 \pm 0.0135$ ,  $\zeta = 0.679 \pm 0.004$ ,  $\xi = 15.871 \pm 8.387$ . It should be noted that the values of  $B, C, \zeta$ , and  $\xi$  are very close for viscosity and conductivity. The graphs in Figs. 4, 5, and 6 show the result of this fitting.

## Conclusion

Our work focused on the quantum study of atomic collisions where the case of the collision of two argon atoms was developed. We have, in a first step, built the potential energy curve along which two fundamental argon atoms approach. This potential was used to solve numerically the radial wave equation and, consequently, determine numerically, for any  $E$  energy and orbital kinetic moment, the phase shifts. In particular, we evaluated the quality of the Ar-Ar potential built by calculating the second virial coefficients. The results we obtained of these coefficients showed their good agreement, mainly at high temperatures, with the values already published. In a second step, we used these phase shifts to quantitatively determine the transport coefficients, diluted gases formed of  $^{40}\text{Ar}$ , by the Chapman-Enskog method. Our

calculations have been expanded to include spin and symmetry effects. Agreement with literature results is demonstrated.

**Acknowledgements** Thanks to Alexey N. Volkov for ab initio data of potential.

**Author contribution** 1 and 2 they wrote the main Manuscripte

3- Figure and table

4- English correction

**Data availability** No datasets were generated or analysed during the current study.

## Declarations

**Conflict of interest** The authors declare no competing interests.

## References

1. Chapman S, Cowling TG (1952) The mathematical theory of non-uniform gases. Cambridge University Press, Cambridge
2. Hirschfelder JO, Curtis CF, Bird RB (1964) Molecular theory of gases and liquids. Wiley and Son Inc, New York
3. Mott NF, Massey HSW (1965) The theory of atomic collisions. Oxford University Press, Oxford
4. Vitaly Petrov A, Omid Ranjbar A, Petr Zhilyaev A, Alexey Volkov N (2020) Kinetic simulations of laser-induced plume expansion from a copper target into a vacuum or argon background gas based on ab initio calculation of Cu-Cu, Ar-Ar, and Ar-Cu interactions. *Phys Fluids* 32:102010. <https://doi.org/10.1063/5.0023784>
5. Sheng X, Peter Toennies J, Tang KT (2020) Conformal analytical potential for all the rare gas dimers over the full range of internuclear distances. *Phys Rev Lett* 125:253402. <https://doi.org/10.1103/PhysRevLett.125.253402>
6. Patkowski K, Murdachaew G, Fou CM, Szalewicz K (2005) Accurate ab initio potential for argon dimer including highly repulsive region. *Mol Phys* 103:2031. <https://doi.org/10.1080/00268970500130241>
7. Margenau H, Walson WW (1936) Pressure effects on spectral lines. *Rev Mod Phys* 8:22. <https://doi.org/10.1103/RevModPhys.8.22>
8. Patkowski K, Szalewicz K (2010) Argon pair potential at basis set and excitation limits. *J Chem Phys* 133:094304. <https://doi.org/10.1063/1.3478513>
9. Zeller S, Kunitski M, Voigtsberger J, Waitz M, Trinter F, Eckart S, Kalinin A, Czasch A, Schmidt LPhH, Weber T, Schöffler M, Jahnke T, Dorner R (2018) Determination of interatomic potentials of He2, Ne2, Ar2, and H2 by wave function imaging. *Phys Rev Lett* 121:083002. <https://doi.org/10.1103/PhysRevLett.121.083002>
10. Geltman S (1969) Topics in atomic collision theory. Academic Press, New York
11. Numerov B (1933) *Publ Observ* 2:188. Central Astrophys. Russ
12. Reichl LE (1984) A modern course in statistical physics. University of Texas Press, Austin
13. Hutem A, Boonchui S (2012) Numerical evaluation of second and third virial coefficients of some inert gases via classical cluster expansion. *J Math Chem* 50:1262–1276. <https://doi.org/10.1007/s10910-011-9966-5>
14. Dymond JH, Smith EB (1980) The virial coefficients of pure gases and mixtures. A Critical Compilation Clarendon, Oxford
15. Blokhintsev D (1981) Principes de mécanique quantique. traduction française, Edition Mir, Moscou

16. Landau LD, Lifshitz EM (1981) Quantum mechanics non-relativistic theory. Pergamon Press, Oxford
17. Ghimire S, Adhikari NP (2017) Study of structural and transport properties of argon, krypton, and their binary mixtures at different temperatures. *J Mol Model* 23:94. <https://doi.org/10.1007/s00894-017-3261-8>
18. Sharipov F, Benites VJ (2019) Transport coefficients of argon and its mixtures with helium and neon at low density based ab initio potentials. *Fluid Phase Equilibria* 498:23–32. <https://doi.org/10.1016/j.fluid.2019.06.010>
19. Song B, Wang X, Liu Z (2015) Recommended gas transport properties of argon at low density using ab initio potential. *Molec Simul* 42:9–13. <https://doi.org/10.1080/08927022.2014.1003296>
20. McQuarrie DA (2000) Statistical mechanics. University Science Books, USA
21. Kestin J, Knierim K, Mason EA, Najafi B, Ro ST, Waldman M (1984) Equilibrium and transport properties of the noble gases and their mixtures at low density. *J Phys Chern Ref Data* 13:229. <https://doi.org/10.1063/1.555703>
22. Atkins PW, De Paula J (2006) Physical chemistry Vol 1: Thermodynamics and kinetics. 8th edn. Oxford University Press, Oxford

**Publisher's Note** Springer Nature remains neutral with regard to jurisdictional claims in published maps and institutional affiliations.

Springer Nature or its licensor (e.g. a society or other partner) holds exclusive rights to this article under a publishing agreement with the author(s) or other rightsholder(s); author self-archiving of the accepted manuscript version of this article is solely governed by the terms of such publishing agreement and applicable law.